Matched-filter acquisition of high-resolution single-shot spirals

Lars Kasper[1,2], Maximilian Haeberlin[1], Saskia Bollmann[1], S. Johanna Vannesjo[1], Bertram J. Wilm[1], Benjamin E. Dietrich[1], Simon Gross[1], Klaas E. Stephan[2], and Klaas P. Pruessmann[1]

[1]Institute for Biomedical Engineering, University of Zurich and ETH Zurich, Zurich, Switzerland, [2]Translational Neuromodeling Unit, Institute for Biomedical Engineering, University of Zurich and ETH Zurich, Zurich, Switzerland

INTRODUCTION Matching MR image acquisition to a targeted post-processing strategy has been shown to yield considerable signal-to-noise (SNR) benefits for fMRI [1]. This matched-filter acquisition method proposes to design a variable density k-space trajectory whose sampling pattern is proportional to the targeted point-spread function of the imaging process – considering all reconstruction as well as post-processing steps, e.g. an applied smoothing kernel. For a matched-filter EPI matching a Gaussian kernel, temporal SNR (tSNR) was found to increase up to 40 % for typical smoothing kernels of 2.5 voxels [1]. In principle, spiral trajectories lend themselves naturally to match rotationally symmetric smoothing kernels, such as the ubiquitous Gaussian kernel, promising an even higher tSNR. However, variable density spiral trajectories are notoriously difficult to use in imaging practice, since they are prone to trajectory imperfections (e.g. eddy currents, heating-induced field drifts) as well as B0 field inhomogeneity [2]. Here, we show how a concerted effort of concurrent magnetic field monitoring, parallel imaging and B0-map-based image reconstruction enables artifact-free high-resolution single-shot spiral acquisition with a Gaussian density.

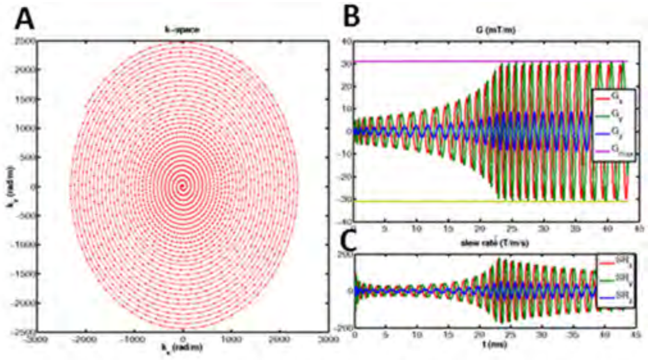

Fig 1. Concurrent Field Monitoring. (A) Measured Trajectory, (B) Gradients and (C) slew rate time course of a matched-filter spiral.

METHODS *Spiral Design* An efficient variable-density weighting can be accomplished by taking an Archimedean spiral readout, but varying trajectory speed, i.e. gradient strength along the trajectory shape. We employed this approach for a 1.25 mm single-shot spiral acquisition with three-fold undersampling that was acquisition-matched to a 2.5 mm FWHM Gaussian smoothing during post-processing. The gradient waveform was determined by an adaptation of the minimum time gradient design algorithm [3] allowing for variable gradient limits in k-space. For comparison, we selected a standard (Archimedean) spiral with the same overall readout time of 45 ms. According to matched-filter theory and simulation, the expected tSNR gains for this matched-filter spiral is about 60 % compared to uniform acquisition, considerably higher than for the reported matched-filter EPI (<40 %).

Imaging Protocol All other imaging parameters were shared between the spiral trajectories, in particular: FOV 230 mm, matrix size 230, resolution 1x1x3mm^{3,} 5 slices, TR 3 s, TE 30 ms, spiral-out acquisition, SENSE-factor 3, 48 volumes per session. Besides, 2 spin-warp gradient echo scans (TE 2/4.23 ms) were acquired with the same geometry parameters for sensitivity and B0-map calculation.

Setup Data was acquired from one female healthy volunteer on a Philips Achieva 3T system and 8-channel Rx-head coil (Philips Healthcare, Best, The Netherlands). Concurrent field monitoring up to 3rd spatial order (k_0, k_x, k_y, k_z, and higher order spherical harmonics) utilized a custom-built setup [4] with 16 ^{19}F-based NMR probes, T/R switches and external RF excitation.

Image Reconstruction and Analysis Image reconstruction employed the concurrent field monitoring data up to 1st spatial order (phase coefficients k_0, k_x, k_y, k_z) in a gridding-based iterative SENSE conjugate-gradient algorithm [5], augmented by multi-frequency interpolation for static B0-correction [6]. To study the impact static B0-correction, all reconstructions were repeated without B0-map information. Temporal SNR was assessed after realignment and smoothing of all volumes in a session using SPM12b, before calculating per-pixel tSNR as mean/std of the time series.

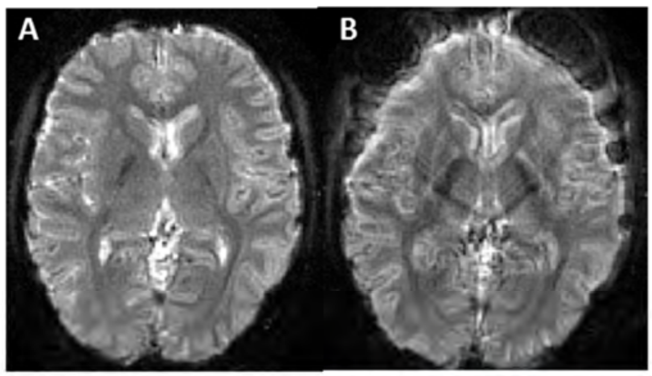

Fig 2. Image Reconstructions of single-shot matched-filter spirals. (A) with static B0 correction. (B) without B0 correction.

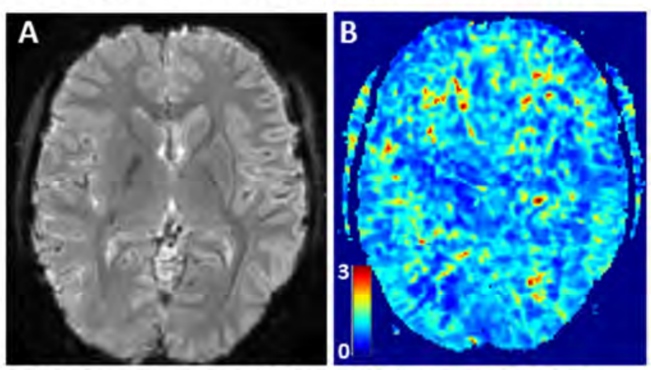

Fig 3. Session Statistics. (A) Mean of 48 dynamics. (B) SNR ratio after smoothing compared to Archimedean spiral.

RESULTS The Gaussian weighting of the matched-filter spiral trajectory could be confirmed by the concurrent monitoring data, in particular the modulation of maximum gradient amplitude over time (Fig. 1a,b). Virtually artifact-free images could be reconstructed from matched-filter spiral acquisition using concurrent field monitoring and B0-map based correction for static field inhomogeneity in the SENSE-reconstruction. (Fig. 2a). However, without B0-correction, no sufficient image quality could be reached (Fig. 2b). The session statistics showed high robustness, as is visible in the ghost-free mean image (Fig. 3a). Also, tSNR improvements could be observed compared to the Archimedean spiral (Fig. 3b). While in some cortical regions, tSNR increased by up to 70 %, especially CSF showed no clear improvements, indicating a considerable influence of physiological noise in the time series.

CONCLUSION High-resolution single-shot variable density spirals with acquisition densities matched to a Gaussian smoothing kernel could be successfully implemented for MRI. Concurrent field monitoring and advanced image reconstruction (iterative SENSE and static B0-correction) proved to be instrumental to arrive at a high image quality. Matched-filter spirals increased tSNR of time series after fMRI-typical post-processing compared to Archimedean spirals and in summary, realizes the best match to Gaussian smoothing kernel to date. This might benefit future applications for high-resolution fMRI that are typically limited by thermal SNR.

REFERENCES [1] L. Kasper *et al.*, *NeuroImage*, 2014, **100**, 145. [2] P. Börnert *et al.*, *MRM*, 1999, **9**, 29. [3] M. Lustig, S.-J. Kim, J.M. Pauly, *IEEE Transactions on Medical Imaging*, 2008, **27**, 866. [4] C. Barmet *et al.*, in *Proc. Intl. Soc. Mag. Reson. Med. 18*, 2010, 216. [5] K.P. Pruessmann *et al.*, *Magnetic Resonance in Medicine*, 2001, **46**, 638—651. [6] B.P. Sutton, D.C. Noll, J.A. Fessler, *IEEE Transactions on Medical Imaging*, 2003, **22**, 178. [7] S.J. Vannesjo *et al.*, *Magnetic Resonance in Medicine*, 2014, **72**, 570.